

NUMERICAL MODELLING OF FREE CONVECTIVE HEAT TRANSFER FROM HEATED PLATES IN AN ENCLOSURE

P.W.CLEARY¹, A.N. STOKES¹, J.G.SYMONS² and P.C. BANDOPADHAYAY²

¹CSIRO Division of Mathematics & Statistics, Clayton, VIC 3168, AUSTRALIA

²CSIRO Division of Building Construction & Engineering, Clayton, VIC 3168, AUSTRALIA

ABSTRACT

A stream function-vorticity-temperature formulation is used with a finite element method to model natural convection. A range of configurations consisting of two parallel heated plates in an isothermal enclosure are modelled. Flow streamlines, velocities, local heat fluxes, isotherms and isofluxlines are calculated. Local heat transfer coefficients and Nusselt numbers are also calculated. The model is in good agreement with the corresponding experimental results over a useful range of Rayleigh numbers.

1. INTRODUCTION

Natural convection occurs in a wide variety of circumstances. It is important for the cooling of micro-electronic circuitry, heating and cooling of buildings and many other industrial devices.

Until recently numerical modelling of such systems, for useful Rayleigh numbers and geometries was not feasible. The improvement in the computational power of computers has now made this possible. Solutions are calculated for the configurations described below. Nusselt numbers, which are a measure of the non-dimensional overall heat transfer rates, and local heat transfer coefficients are calculated and compared with the appropriate experimental results contained in Symons *et al.* (1987, 1988 and 1991).

2. THE PHYSICAL CONFIGURATION

The physical configuration being modelled is a pair of identical parallel plates of length $L = 150$ mm. They are placed in the geometric center of a 600 mm square isothermal enclosure. The aspect ratio A of the pair of plates is the ratio of the center to center spacing of the plates to their length L . The plates are either 10 or 16 mm thick. The 10 mm plates are solid. The 16 mm plates consist of two separate 6 mm plates separated by a 4 mm insulating layer. This allows the overall heat transfer from each side of each plate to be measured.

The plates are heated and maintained at a temperature of 55°C and the enclosure cooled and maintained at 40°C . The angle of inclination of the pair of parallel plates is varied between horizontal and vertical.

The Rayleigh number (Ra) is based on the length of the plates and the temperature difference between the heated and cooled surfaces. This is the same scaling as used in the experimental results.

3. MATHEMATICAL MODELLING

The scaled equations of motion for steady state natural convection in two dimensions are:

$$\mathbf{v} \cdot \nabla \mathbf{v} = -\nabla P + \nabla^2 \mathbf{v} + \left(\frac{Ra}{Pr}\right) T \mathbf{g} \quad (1)$$

$$\text{div } \mathbf{v} = 0 \quad (2)$$

$$Pr \mathbf{v} \cdot \nabla T - \nabla^2 T = 0, \quad (3)$$

where Ra is the Rayleigh number and Pr is the Prandtl number. \mathbf{g} and \mathbf{k} are the unit vectors in the direction of gravity and normal to the (x, y) plane. We define the stream function ψ by $\mathbf{v} = \text{curl}(\psi \mathbf{k})$. The vorticity is given by $\omega = \mathbf{k} \cdot \text{curl } \mathbf{v}$ and the equations of motion can be rewritten as:

$$\text{curl}(\psi \mathbf{k}) \cdot \nabla \omega - \nabla^2 \omega - \left(\frac{Ra}{Pr}\right) \frac{\partial T}{\partial x} = 0 \quad (4)$$

$$\omega + \nabla^2 \psi = 0 \quad (5)$$

$$Pr \text{curl}(\psi \mathbf{k}) \cdot \nabla T - \nabla^2 T = 0. \quad (6)$$

The non-slip velocity boundary conditions are:

$$\psi = \text{constant}, \quad \frac{\partial \psi}{\partial n} = 0.$$

For the outside enclosure $\psi = 0$. The temperature boundary conditions are $T = 0$ on the enclosure and $T = 1$ on the plates.

For most of the vertical and horizontal plate cases the configuration is symmetric. The solution is only calculated in the left half of the computational domain. The boundary condition

$$\psi = \omega = \frac{\partial T}{\partial x} = 0.$$

is applied on the line of symmetry.

The solution technique is a Galerkin Finite Element Method using unstructured simplex meshes. Details of the method and its implementation are given in Stokes *et al.* (1991). The computational domain is divided into a triangular mesh, which is concentrated along the outer boundaries and particularly along the sides of the plates in order to resolve the very thin boundary layers and steep temperature gradients present at high Ra .

The nonlinear convective term is dealt with using an explicitly quadratically convergent Newton Raphson technique. The resolution of the mesh determines the smallest boundary layer thickness that can be resolved and hence the highest Ra for which a steady state solution can be found. Typically between 2,500 and 4,000 corner nodes are used, resulting in 25,000 to 50,000 equations to solve. This is presently performed using a direct LU decomposition.

The fully enclosed body represents a particular challenge. The stream function is required to be constant, but the value of the constant Ψ is unknown. In the FEM representation, suppose the nodal values around the body or island are $\psi_1, \psi_2, \dots, \psi_N$ then the condition of constancy for the streamfunction gives N equations; $\psi_2 = \psi_1, \psi_3 = \psi_2, \dots, \psi_N = \psi_{N-1} = \Psi$ in $N+1$ unknowns. Ψ is related to some average of the values at neighbouring nodes. In order to avoid producing long columns in the global matrix this is formulated locally as $\psi_{i+1} = \psi_i + \epsilon(\psi_i - \langle \psi_l \rangle)$. Here $\langle \psi_l \rangle$ is some average of local non-boundary nodes and epsilon is small. This gives a soluble system of $N+1$ local equations in $N+1$ unknowns

The Nusselt numbers are calculated by normalising the integrated heat flux from each body or surface with the heat flux from the conduction case, which is approximated by the $Ra = 1$ value. Here $Pr = 0.71$.

4. FLOW PATTERNS

Cases designated AA, AB, AE and AF are 10 mm thick plate pairs that are vertical, horizontal, and inclined at 15° and 30° to the horizontal, respectively. Only overall Nu for each plate are available experimentally for these cases. Cases AK, AL and AM are 16 mm thick plate pairs that are vertical, horizontal and inclined at 45° respectively. Nu are available for the inner and outer surface of each of these plates.

Figure 1 shows a typical fluid and heat flow patterns for the horizontal 10 mm thick case (AB) at $Ra = 3 \times 10^6$. At this relatively high Ra the flow is characterised by very high temperature gradients around the plates, (Fig. 1b), a strong plume and very thin boundary layers around both the outer walls and the plates, (Fig 1a). Near the plates the flow closely follows the surfaces. There is no through flow between the plates. The flow does, however, penetrate between the plates. It enters from either side, flows along the top surface of the bottom plate and rises from the middle of this surface to the bottom surface of the top plate. It returns in the direction opposite to that from which it entered. It then travels along the top surface of the top plate. The plume finally separates from the top plate near the center. It rises vertically until it reaches the top of the enclosure and is forced to recirculate by the outer walls. The fluid travels down to the lower left corner. Here it encounters the relatively cool, quiescent fluid at the bottom. The plume is still warmer and so again rises vertically, before cooling sufficiently and moving along an oscillating path back to the plates. This is shown clearly by the velocity field in Fig 1d. The isofluxlines, (Fig 1c), show the behaviour of the heat flow. Note the existence of closed isofluxlines.

The imposition of symmetry does not affect the flow patterns or the heat transfer. Using a full width configuration and perturbing the symmetry slightly by inclining the plate 1° causes the plume to separate from the plate about two thirds of the way along instead of in the center. There is still no through flow between the plates. This variation has a negligible effect on the Nu for the entire calculated range of Ra.

The overall flow patterns, (away from the plates), for all these different configurations, regardless of angle of inclination or the aspect ratio are broadly similar, at the same Ra. The specific behaviour of the flow as Ra is increased from 1 to 2×10^6 , for the 10 mm vertical plate case AA is discussed in Cleary *et al.* (1992).

The variation in plate geometry principally affects the flow patterns in the immediate vicinity of the plates. The flow throughout the rest of the enclosure is almost entirely determined by the geometry of the enclosure and shows little change with the specific details of the plates. Changes in angle make the plume somewhat asymmetric, rising from the higher end to the middle of the top wall of the enclosure. One recirculation region is slightly larger than the other.

The maximum Ra attainable numerically is of the order $2-4 \times 10^6$. Here eddy like recirculations begin to form and the flow becomes unsteady for higher Ra. This appears to be a genuine physical phenomena and not a numerical convergence problem resulting from lack of resolution in the mesh. If too coarse a mesh is used convergence cannot be achieved at lower Ra.

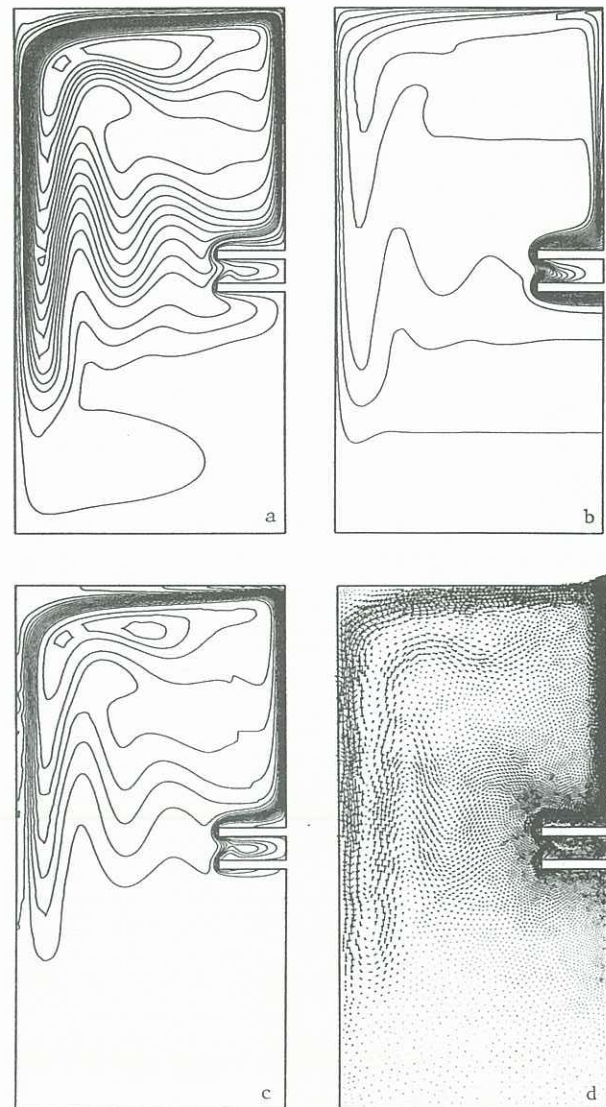


Figure 1 : Numerical flow predictions for $Ra = 3 \times 10^6$, (a) streamlines, (b) isotherms, (c) isofluxlines, (d) local fluid velocities.

5. COMPARISON OF HEAT TRANSFER RATES

Experimental determination of flow patterns is very difficult. The characteristics that can more easily be measured and thus compared are the local heat transfer coefficients and overall heat transfer rates represented by the dimensionless Nusselt numbers.

Figure 2 shows the overall Nu of the pair of plates for seven different configurations with $A = 4$. The vertical AA and AK curves are very similar as are the horizontal AB and AL cases. The 30° inclined 10 mm case and the 45° inclined 16 mm case are indistinguishable, showing that the heat transfer is also relatively insensitive to inclination, once it is beyond about 25°. This observation is consistent with the experimental observations (Symons, Private Communication). The 15° inclined 10 mm case is at sufficiently shallow an angle that its Nu curve lies midway between the horizontal and the 30° inclined case. All the curves fit neatly into the narrow envelope formed by the limiting horizontal and vertical cases. For the range of Ra calculated, the thickness of the plates has little effect on the heat transfer regardless of the angle of the plates.

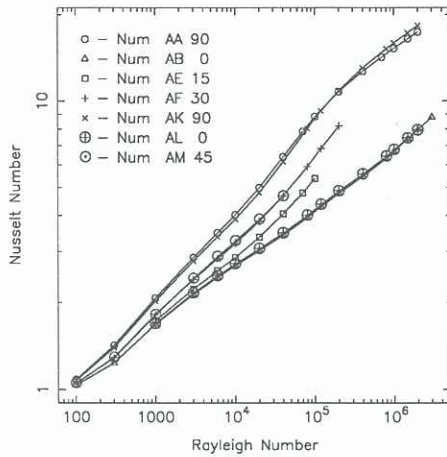


Figure 2 : The overall Nu for 10 mm and 16 mm plates at angles ranging from vertical to horizontal.

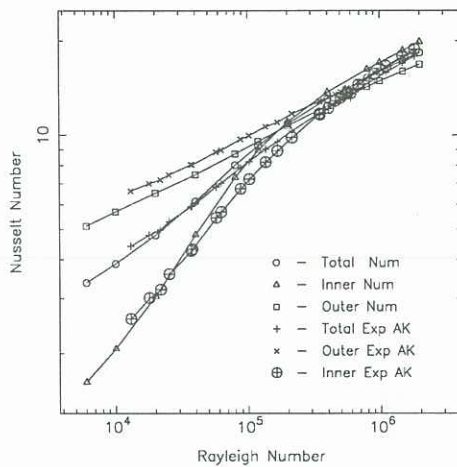


Figure 3 : Comparison of overall, inner and outer face numerical and experimental Nu for a pair of parallel 16 mm vertical plates.

There are very close similarities between the numerical and experimental Nu for each of the inner and outer face Nu and for the overall Nu. These are shown in Figure 3. Each numerical Nu curve has the same shape and magnitude as the experimental one. Not only are the magnitudes in close agreement, the behaviour with varying Ra is also in very close agreement. The Ra for which the inner and outer face Nu curves intersect, (here the inner face begins contributing more to the heat transfer than the outer one), is also in close agreement.

At $Ra = 2 \times 10^6$ the experimental curves are bounded closely by the numerical ones. This results from an experimental averaging effect, where some heat leaks through the insulating layer between the two sides of the plates.

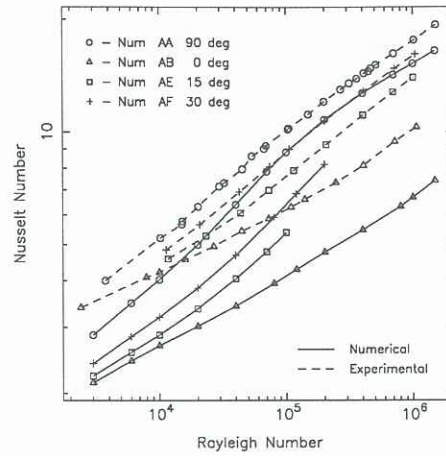


Figure 4 : Comparison of overall numerical and experimental Nu for 10 mm parallel plates at angles ranging from vertical to horizontal.

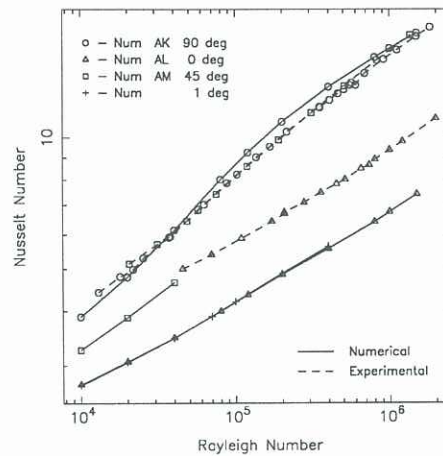


Figure 5 : Comparison of overall numerical and experimental Nu for 16 mm parallel plates at angles ranging from vertical to horizontal.

Figures 4 and 5 show the numerical and experimental results for the 10 mm cases and the 16 mm cases respectively, for various inclinations and $A=4$. There is very close agreement between the numerical and experimental results for the two vertical cases AA and AK. The numerical Nu curves for the inclined cases AE, AF, and AM qualitatively similar to the experimental ones, they have the same shape, but differ in magnitude by about 20%. The horizontal cases AB and AL again are qualitatively similar, (the numerical and experimental curves are again parallel), but these differ in magnitude by about 30%. The experimental flow for horizontal plates is much less steady than the flow for vertical plates and so has larger uncertainty. Here we are comparing steady state solutions with time averaged unsteady ones, so some differences are not surprising.

Figure 6 shows the inner, outer and overall Nu for three different aspect ratios of 10 mm vertical parallel plates. The outer face Nu curve, (the upper one), varies little as the plates are moved closer together. There is, however, a substantial decrease in the inner face Nu, (the lower one).

As the aspect ratio A increases the point at which the inner face makes a significant contribution to the overall heat transfer occurs at higher Ra . The difference between the overall Nu curves, (the middle ones), is smaller and results entirely from the variable contribution from the inner face.

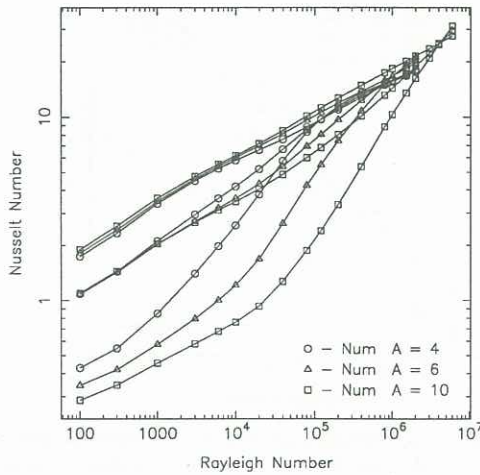


Figure 6 : Comparison of overall, inner and outer face numerical Nu for three different plate separations $A = 4, 6, 10$ using 10 mm vertical plates.

Figure 7 shows the local heat transfer coefficient for the faces of the plates. Fig 7b and 7d are the horizontal plate cases and show only the one half of the length of the plate. The curve is always symmetric about $d = 1/2$. (a) shows that the inner face has higher heat transfer than the outer face except at the very bottom of the plate. These curves are close to the $1/4$ power law for heat transfer from a single plate in an infinite enclosure.

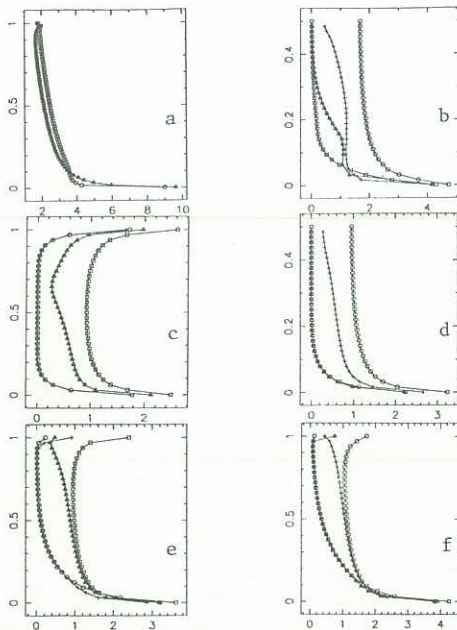


Figure 7 : h_c (horizontal axis), for inner and outer faces of the plates as a function of distance from the plate bottom. (a) AA at $Ra=2 \times 10^6$, (b) AB at $Ra=2 \times 10^6$, (c) 1° inclined case at $Ra=10^5$, (d) AL at $Ra=10^5$, (e) AE at $Ra=10^5$, (f) AF at $Ra=10^5$.

For Figure 7b the curves from left to right are for the bottom face of the top plate which contributes little, except at the very corners. The top face of the bottom plate contributes to h_c for 20% of the length at either end. The top face of the top plate contributes along its entire length but with a minimum in the center. The most efficient heat transfer occurs all along the bottom face of the bottom plate with maxima at either end. Comparing (c) and (d) we find the two inner faces (with curves together on the left) contribute negligibly. The next two curves belong to the top face of the top plate and the bottom face of the bottom plate. The magnitude of these curves are the same for both (c) and (d). The only difference is the position of the minimum on the top face curve. For the 1° inclined case it has moved 20% along the plate. This is the point at which the plume rises. Figures 7(e) and (f) are for inclined plates. The shape of these curves is a combination of that found in both the horizontal and vertical plate cases. The 30° inclined case has a slightly greater maximum at the lower end, otherwise these two cases are very similar.

CONCLUSIONS

Natural convective phenomena can be modelled at useful Ra . The flow patterns found for all the different configurations, regardless of angle of inclination or their aspect ratio are broadly similar, at the same Ra . The detailed differences occur mostly near the plates. The main effect of inclination is to make the plume slightly asymmetric and for one recirculation region to be slightly larger than the other. Even the streamline oscillations returning to the plate are similar.

The Nu curves for the vertical plate curves, both overall and for the inner and outer faces, are in very close agreement with the experimental curves. The inclined plate and horizontal plate cases are qualitatively very similar, (the curves are almost parallel), but differ in magnitude by about 20% and 30% respectively. Moving vertical plates closer together has no significant effect on the heat transfer from the outer faces, but substantially reduces the heat transfer from the inner faces. This is due to throttling of the flow between the plates.

REFERENCES

- CLEARY, P. W., BANDOPADHAYAY, P. C., and SYMONS, J. G., (1992), Numerical modelling of free convection in an electronic cooling application, *Proc. NSF/DITAC Workshop on Thermal Conductance Enhancement in Microelectronics*, Melbourne, 4th - 7th May.
- STOKES, A. N., CLEARY, P. W., THOMPSON, M. C., WELSH, M. C. and HOURIGAN, K., (1991), Finite element methods and applications for fluids on unstructured simplex meshes. *Proc. 5th International Conference on Computational Techniques and Applications*, Adelaide, 15th - 17th July.
- SYMONS, J. G., MAHONEY, K. J., and BOSTOCK, T. C., (1987), Natural convection in enclosures with through flow heat sources, *Proc. ASME-JSME Thermal Engineering Joint Conference*, Honolulu, 22th - 27th March, pp 215-220.
- SYMONS, J. G., MAHONEY, K. J., and BOSTOCK, T. C., (1988), Convective heat transfer from heated plates in a sealed enclosure: The application to printed circuit boards, *Proc. MECH 88, The Institute of Engineers*, Australia, Brisbane, 8-13 May, pp. 84-88.

- SYMONS, J. G., WHITE, R. F., and MEDDINGS, S. J., (1991), Natural convection through parallel plate arrays, *Proc. 4th International Symposium on Transport Phenomena in Heat and Mass Transfer*, Sydney, 14th - 19th July, pp. 95-106.